



Development of Oil Palm Shell-reinforced 316L Stainless Steel Composite Prepared by Powder Metallurgy Route

Zulaikha Abdullah^{1*}, Che Susilawati Che Berahim¹

¹Jabatan Kejuruteraan Mekanikal, Politeknik Mukah (PMU), KM 7.5, Jalan Oya, 96400, Mukah, Sarawak, Malaysia

*Corresponding author: zulaikha@pmu.edu.my

Please provide an **official organisation email** of the corresponding author

Full Paper

Article history

Received

15 June 2022

Received in revised form

15 June 2022

Accepted

20 June 2022

Published online

15 July 2022

Abstract

Metal matrix composite (MMCs) gained interest of researchers over the past decades due to demand for excellent and stiff materials. MMCs offer several advantages like high specific strength and modulus, improved elevated temperature properties, low coefficient of thermal expansion, enhanced electrical performance, wear and abrasion resistance. 316L Stainless steel composite was prepared by powder metallurgy route. Stainless steel type 316L acting as metallic powder was mixed with Polyvinyl Alcohol (PVA) and Oil Palm Shell (OPS) as reinforcement. Then, physical observation and shrinkage percentage of the resulting samples was analysed. From the result, the observational best results were shown by 55 wt. % stainless steel samples as porosity are present and their ability to maintain the cylindrical shape of the compacted sample.

Keywords: - metal matrix composite, stainless steel, sintering, shrinkage

© 2022 Politeknik Mukah. All rights reserved

1. Introduction

The composite material can be defined as a combination of two or more materials with appropriate physical and chemical properties which produce material with better properties compared to its individual constituents (Deshpande, 2019). In the recent decade, extensive research is focused on metal matrix composites (MMCs) due to demand in a high-performance application such in automobile, aerospace, and manufacturing industries (Annaraj et al., 2019). MMCs are a combination of two phases which are matrix phase and reinforcement phase. The main advantages of MMCs are high strength and stiffness, low thermal stress, electric conductivity, and wear resistance (Alem et al., 2020). Other than casting methods, powder metallurgy is a promising method to produce MMCs. The powder metallurgy route consists of three main processes, mixing

of the metallic and reinforcement materials, compaction process, and sintering process.

In this research, 316L Stainless steel composite is produced by using powder metallurgy route. The powder of stainless-steel type 316L is used as metallic material, Oil Palm Shell (OPS) used as reinforcement and Polyvinyl Alcohol (PVA) as binder. All the materials are mixed homogeneously by using a roller mixing machine. After that, the mixtures are poured into the cylindrical mould to be compacted using a uniaxial pressing machine. After the samples are compacted, the samples are then sintered in two stages by using a tube furnace at temperature of 1150°C. The physical observation and shrinkage of the samples were studied after the sintering process.

2. Literature Review

MMCs offer a good combination of properties such as high strength to weight ratio, low thermal expansion coefficient, great wear resistance, and abrasion resistance. MMCs are most popularly used in aerospace, automobile, rails transport, marine, and army sector applications. MMCs fabrication method can be classified into two which are liquid phase processing and solid-state processing. Liquid phase processing can be defined as the process of producing MMCs by mixing the discontinuous reinforcement phase into the continuous metal matrix phase in the liquid state. Solid-state processing methods produced MMCs below the melting temperature of the matrix (Sharma et al., 2019).

Historically, Powder Metallurgy route first discovered was about 3000 BC when Egyptians used iron ores to make tools. Powder metallurgy is the most common technique to produce MMCs. Major advantages of powder metallurgy route are providing a cost-effective shaping process, with virtually no loss of material, to mass produce components with close dimensional precision and required mechanical properties (Tan et al., 2020). In powder metallurgy technique, the metallic and reinforcement powder will be mixed and compacted to produce a green body before proceeding to a further process which is the sintering process. In the sintering stage, the temperature below its melting temperature (T_m), usually $0.6 - 0.9 T_m$ will be selected to make a uniform dense resulting structure (Alem et al., 2020).

Stainless steel is an outstanding achievement of modern metallurgy because of its outstanding near net shape and high raw materials utilisation. (Li et al., 2020). It has been noted that the main difference between stainless steels and other steels is that the former has a few nanometer layers of chromium oxide on the surface while the later form iron oxides as shield to prevent from corrosion happen to the surface of the metal (Abdullah et al., 2018). Thus, 316L stainless steel composite is promising due to its excellent corrosion resistance and great mechanical properties (Patel et al., 2019).

The oil palm, specifically the species of *Elaeis Guineensis*, has historically been cultivated in tropical Africa's semi-wild areas. Based on a research by Chizari in 2017, an estimation of palm oil yield will continue to increase from 2015 to 2020. Nevertheless, the presence of these oil palm wastes has created a major disposal problem. One of the solid wastes that is produced by the oil palm industry is the palm oil kernel or also known as oil palm shell (OPS) (Chizari et al., 2017). There are multiple uses of OPS in the engineering field. It has been used as activated carbon in textile wastewater treatment, bio composite in polymer industry, concrete pavement, biomass gasification and combustion fuel for steam generation. Activated charcoal prime use is as an absorbent and has many applications. One of its main applications is for contaminant removal from water and gases (Yahayu et al., 2018).

3. Methodology

Stainless steel 316L powder with size $7.2 \mu\text{m}$ act as metallic powder was mixed with Oil Palm Shell (OPS) as reinforcement material and Polyvinyl Alcohol (PVA). Stainless steel 316L powder supplied by Maju Scientific Sdn. Bhd. OPS was collected from Bukit Lawiang Kluang Palm Oil Mill, Johor. The composition of stainless steel used were 55, 60, 65, 70, 75 and 80 weight percent (wt. %) and the remaining for reinforcement material. The amount of PVA used is fixed at 5 weight percent (wt.%) for all composition.

OPS was crushing using the Fritsch Variable Speed Rotor Mill PULVERISETTE 14 crushing machine. All the material was sieved using a Fritsch sieving machine with the sieving filter arranged following the sequence starting from $600 \mu\text{m}$, $400 \mu\text{m}$ and $200 \mu\text{m}$, and mixed using a roller mixing machine at 100 RPM for 30 minutes. The mixture was carefully poured into a cylindrical mould and compacted at pressure 6 tons with 10 minutes holding time. The sample was sintered at temperature 1150°C using a tube furnace. The samples are heated in a furnace for 3 hours at a rate of 2°C per minute and are maintained at 470°C for 3 hours. This stage would cause a reaction where the OPS particles and stainless-steel powder would be able to bind since the binder would melt at 60°C for the purpose of holding the sample shape. The sample is then heated again to melt the stainless-steel powder at the same rate of heating until a temperature of 1150°C is achieved and is maintained for one hour. No more increase of temperature is done after this stage and the samples are allowed to be cooled at a rate of 2°C per minute. The graph of temperature vs time is as Figure 1.

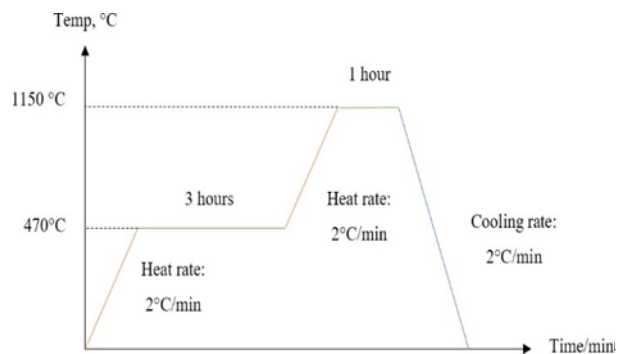


Figure 1. Profile sintering temperature of the sample

Then, the samples were analysed for their physical observation and shrinkage percentage. The physical condition of the samples will be observed using the naked eye to identify the surface condition and is recorded to compare the before and after sintering. Observations will focus on the cracks, colour changes on the surface and physical form of the samples. The durability of the samples is then observed by touching the samples to identify the hardness.

The thickness of the samples is compared to measure the shrinkage percentage. The height is recorded using a

digital calliper for accuracy. The height before sintering is first recorded and changes in height after sintering is then compared with these results. The change in height is then calculated as the shrinkage percentage. The method of shrinkage percentage of sample calculations is shown below:

$$\text{Shrinkage (\%)} = \frac{h_{\text{initial}} - h_{\text{sintered}}}{h_{\text{initial}}} \times 100 \quad (1)$$

where;

$h_{\text{initial}} = h_{\text{initial}}$ = sample height before sintering

$h_{\text{sintered}} = h_{\text{sintered}}$ = sample height after sintering

4. Finding and Analysis

Before the sample is sintered, as shown in Figure 2 (a), the sample shows a shiny surface with the OPS granule present in the sample as grey colored as if it was mixed with the stainless steel 316L powder. Small cracks can be seen from the outer surface while showing a shiny surface due to the SS316L powder. After sintering, porosity can be seen on the surface of the sample as shown in Figure 2(b). The post-sintered samples still retain the cylindrical shape while the porosity shows the presence of burned OPS. The samples darken to black in colour and little distortion can be seen on the sample shape as seen in Figure 2 (b), where the SS316L powder was melted at the upper part of the sample.

Referring to Figure 2(c), before sintering shows a shiny surface with grey colour from the stainless steel and granules from the presence of OPS grains. Small cracks are visible, and the surface is shiny due to the presence of SS316L powder bonded with the PVA. The pre-sintered samples were fragile and extra attention was needed during. Referring to Figure 2(d), shown that they are still able to maintain the cylindrical shapes with porosities being visible on the surfaces. From the results, it is shown that large pores on the surface while having melted SS316L solids, with shiny silver surfaces. The shiny silver surface formed due to the location of this sample placed in the tube furnace during the sintering process is near to the argon passage to make this sample get sufficient argon gas during the sintering process. It is also able to maintain most of its original cylindrical shapes.

As shown in Figure 2(e), the sample before sintering is cylindrical in shape and grey in colour with visible OPS granules on the surface. Fine cracks can be seen on the surface with shiny grey colour on the surface of the sample. The sample is very fragile at this state and extra care was given during storage. Based on figure 4.8, the sample has darkened into black colour after sintering. The porosity can be seen with the presence of burned OPS grain. Sample in Figure 2(f) shows a slightly larger pores and the cylindrical shape is still visible. The surface is mostly melted into solid SS316L as seen on Figure 2(f).

From Figure 2(g), the sample is shiny grey and shows the presence of the OPS on the pre-sintered sample.

Compaction causes the sample to be held together by the PVA binder and the height was recorded. Referring to Figure 2(h), the sample shown shows large porosity with some grains of burned OPS within it. Both samples darkened to black colour after sintering and were completely hardened.

Before sintering, the sample is shiny grey and shows the presence of the OPS content within it in granule form as shown in Figure 2(i). Tiny cracks are present with the outer surface of the sample being shiny silver in colour. From Figure 2(j), the sample has darkened into black colour while having small pores. The shape had distorted but still visibly shows the cylindrical shape of pre-sintering. The sample shows more porosity while having a shiny silver surface solidified and shows melted SS316L when being touched by hands and is not fragile.

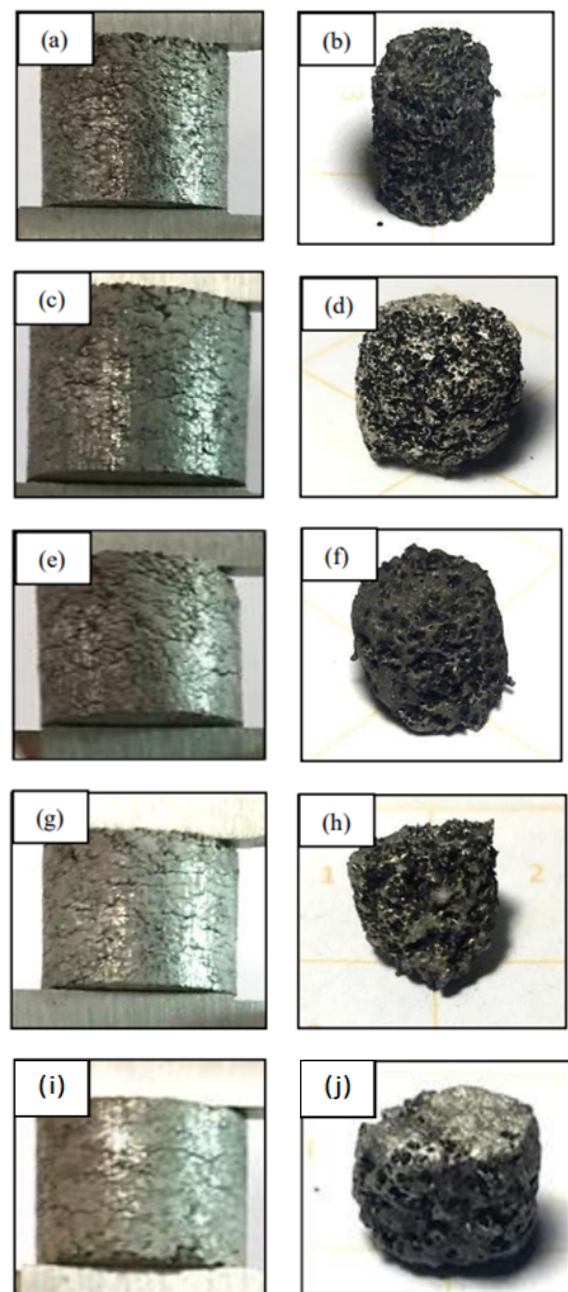


Figure 2. (a) shows 55wt. % SS samples before sinter, (b) shows 55wt. % SS samples after sinter, (c) shows 60wt. % SS samples before sinter, (d) shows 60 wt. % SS samples after sinter, (e) shows 65wt. % SS samples before sinter, (f) shows 65wt. % SS samples after sinter, (g) shows 70 wt. % SS samples before sinter, (h) shows 70 wt. % SS samples after sinter, (i) shows 75wt. % SS samples before sinter, and (j) shows 75wt. % SS samples after sinter

Figure 3 shows a graph of the selected samples to be analysed for the average shrinkage. Each sample is calculated for their shrinkage value and is then used to calculate the average shrinkage of each stainless-steel composition. Highest value of each sample is shown by 55 wt. % at 44.63% shrinkage while the lowest is shown by 75 wt. % at 25.1% shrinkage. The average shrinkage values from this table is then used to generate the chart in Figure 3 to clearly see the trendline of shrinkage percentage changes along the stainless-steel composition.

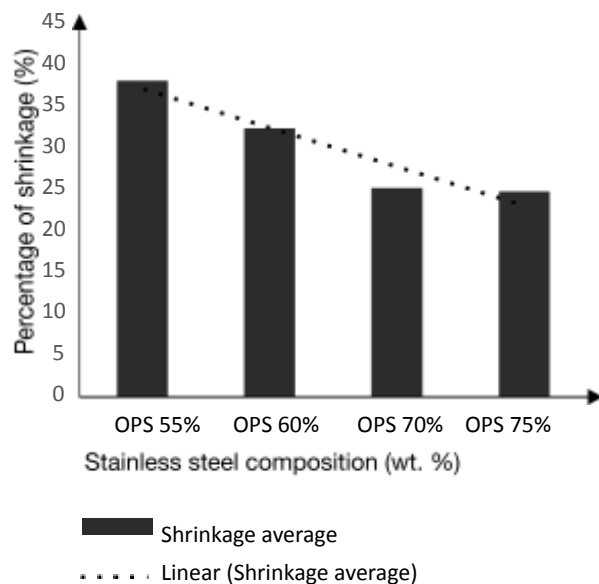


Figure 3. Graph of percentage of shrinkage of sample height for selected samples

From Figure 3, the highest shrinkage is shown by 55 wt. % with 38.21% shrinkage. The data proves that the high composition of OPS causes the sample to shrink the most. The OPS is burned, and the spaces occupied by OPS are then turned into pores. Stainless steel powder solidifies and retains the cylindrical shape. 75% wt. % of stainless steel shows the least shrinkage with only 24.89%. This is due to the high content of stainless steel 316L powder and the least amount of OPS in the sample. Least amount of porosity can also be seen in 75% sample as seen in Figure 2(j) The porosity can be compared with Figure 2(b) where the sample shows higher porosity. Insignificant comparison 70 and 75 wt. % may be due to a sample at 65 wt. % is not present in the graph.

There were also multiple failures in the sample retaining the cylindrical shape. This is due to the binder

composition not suitable since the PVA binder is fixed at 5 wt. % for this study. The quantity and concentration of the binder is critical and should be selected appropriately so as to optimise the mixing process and obtain a homogeneous mixture of metal matrix powder and reinforcement particles. Most samples were black in colour and did not maintain the initial cylindrical shape. The colour change was caused by oxidation during sintering. Sample failures may also be due to other elements existing during sintering that may be present inside the tube furnace.

Overall, 55 wt. % shows the highest potential for further study since it shows the highest porosity and the best in retaining their initial green sample shape. 55 wt. % or lower is suitable to be sintered at this temperature by using a tube furnace.

5. Conclusion

Green compact of all samples were successful as the sample was able to maintain the cylindrical shape with mass of 5 grams. The compacted samples were measured carefully to avoid breakage as the samples were fragile. After sintering, the best results were shown by 55 wt. % stainless steel samples as porosity are present and their ability to maintain the cylindrical shape of the compacted sample. Most samples are black in colour and are varying in shape such as elliptical and separated solids while only 2 samples had failed and formed into powder form. The change in colour was due to oxidation during sintering of the samples. The amount and composition of the binder is essential and should be chosen in order to maximise the binding phase and to achieve a homogeneous mixture of metal matrix powder and reinforcement particles.

The height change post-sintering was increasing as the SS316L content was increasing. The shrinkage percentage is decreasing as the SS316L content is increasing which shows that the higher the OPS content, the lower the height change after sintering. Altogether, 55 wt. % shows the highest potential for further study as it shows the highest porosity and best ability to retain the original green sample shape. 55 wt. % or lower is ideal for sintering at this temperature by means of a tube furnace. The suitability of sintering temperature, binder wt. % and type of furnace should be investigated further for samples of 60 wt. % and above since most samples range from 60% to 80 wt. % Hardly able to maintain the cylindrical shape and little porosity is shown.

Acknowledgment

Authors would like to acknowledge the support from the Malaysia Ministry of Education for financial support through the MyBrain15 scholarship under MyPhD program.

References

- Abdullah, Z., Ahmad, S., Ismail, A., & Ahmed Khan, N. (2018). Processing of porous stainless steel by compaction method using egg shell as space holder. In *Key Engineering Materials* (Vol. 791).
- Alem, S. A. A., Latifi, R., Angizi, S., Hassanaghaci, F., Aghaahmadi, M., Ghasali, E., & Rajabi, M. (2020). Microwave sintering of ceramic reinforced metal matrix composites and their properties: a review. *Materials and Manufacturing Processes*, 35(3), 303–327.
- Annaraj, J. P., Bose, N., & Rajesh Jesudoss Hynes, N. (2019). A review on mechanical and tribological properties of sintered copper matrix composites. *AIP Conference Proceedings*, 2142(August).
- Chizari, A., Mohamed, Z., Shamsudin, M. N., & Seng, K. W. K. (2017). Economic Climate Model of the Oil Palm Production in Malaysia. *International Journal of Horticulture, Agriculture and Food Science*, 1(3), 27–32.
- Deshpande, M. (2019). Design and Performance of Ball Milling for Powder Metallurgy Composites. 7(07), 1–3.
- Li, Z., Ni, H., Chen, Z., Ni, J., Chen, R., Fan, X., Li, Y., & Yuan, Y. (2020). Enhanced tensile properties and corrosion resistance of stainless steel with copper-coated graphene fillers. *Journal of Materials Research and Technology*, 9(1), 404–412.
- Patel, M., Muthu Vaidyanathan, R., Sivaraman, N., Markos, M., & Alemayehu, T. (2019). Microstructure and microhardness of ZrO₂ reinforced PM 316L austenitic stainless-steel composites sintered in ambient and argon atmosphere. *International Journal of Engineering and Advanced Technology*, 8(6), 38–42.
- Sharma, D. K., Mahant, D., & Upadhyay, G. (2019). Manufacturing of metal matrix composites: A state of review. *Materials Today: Proceedings*, 26(2020), 506–519.
- Tan, Z. qiang, Zhang, Q., Guo, X. yi, Zhao, W. jiang, Zhou, C. shang, & Liu, Y. (2020). New development of powder metallurgy in automotive industry. *Journal of Central South University*, 27(6), 1611–1623.
- Yahayu, M., Abas, F. Z., Zulkifli, S. E., & Ani, F. N. (2018). Utilization of Oil Palm Fiber and Palm Kernel Shell in Various Applications. *Sustainable Technologies for the Management of Agricultural Wastes*, 45–56.